International Journal of Computational Methods

ANISOTROPIC DAMAGE MODELS FOR GEOMATERIALS: THEORETICAL AND NUMERICAL CHALLENGES

HAO XU*,† and CHLOÉ ARSON*,‡

*School of Civil and Environmental Engineering,
Georgia Institute of Technology,
Atlanta, Georgia 30332, U.S.A.
Center for Tectonophysics, Texas A&M University
†haoxu@gatech.edu
‡chloe.arson@ce.gatech.edu

Received (Day Month Year)
Revised (Day Month Year)

A new anisotropic damage model for rock is formulated and discussed. Flow rules are derived with the energy release rate conjugate to damage, which is thermodynamically consistent. Drucker-Prager yield function is adapted to make the damage threshold depend on damage energy release rate and to distinguish between tension and compression strength. Positivity of dissipation is ensured by using a non-associate flow rule for damage, while non-elastic deformation due to damage is computed by an associate flow rule. Simulations show that the model meets thermodynamic requirements, follows a rigorous formulation, and predicts expected trends for damage, deformation and stiffness.

Keywords: geomaterials, Continuum Damage Mechanics, crack-induced anisotropy, multi-mechanisms, thermodynamic framework, stiffness, damage criterion, flow rule

1. Introduction

Continuum Damage Mechanics (CDM) initially aimed to predict deformation and stiffness in solids subject to cracking. The increasing need for high-performance cement-based materials in construction, and the new challenges associated to deep geological storage, raised interest in studying the behavior of quasi-brittle geomaterials such as concrete and rock. Geomaterials have a heterogeneous porous structure needing rigorous characterization by *ad hoc* parameters, in order to determine the "reference state", i.e. the mechanical state in which the material is considered undamaged. Porous networks are generally complex, especially in microporous rock such as coal and shale, which comprise flaws ranging from the nanoscale to the millimeter scale [Loucks *et al.* (2009)]. Extending the framework of CDM to geomechanics thus raises many theoretical issues associated to the multiple scales of observation that need to be considered. Micro-mechanics allows predicting the initiation and propagation of individual defects. Sophisticated homogenization schemes were proposed in order to upscale material properties at the

scale of a Representative Elementary Volume (REV) of rock [Pensée *et al.* (2002); Guéry *et al.* (2008)], including saturated cases [Dormieux *et al.* (2006)] and non-local damage effects [Zhu *et al.* (2007)]. Assumptions have to be made on the shape of the cracks. Models were often restricted to the growth of cracks having the same shape, orientation and growth rate. In theory, micro-mechanical models could predict the evolution of as many kinds of defects and defect orientations as needed, as long as evolution laws can be provided. The CDM thermodynamic framework is well-suited for numerical implementation in Finite Element Methods (FEM) because discontinuities are modeled as energy losses at the REV scale.

The fabric (or "morphology") of the intact medium has a strong impact on damage evolution in granular media such as concrete and rock, and even in composites. Voronoi cell FEMs were used to predict the influence of microstructure on crack propagation [Li and Ghosh (2004)] in a medium containing stress-induced heterogeneities. Extended Finite Element Methods (X-FEM) were used to predict fracture propagation in homogeneous and layered media including composites with delamination [Nagashima and Suemasu (2006)]. However, modeling the damaged zone ahead of the fracture tip, as would be of interest for rock subject to hydraulic fracturing or shear faulting for instance, still raises many issues related to the difficult modeling of the transition between damaged continuum and discontinuous medium [Mazars and Pijaudier-Cabot (1996)]. Several numerical methods were proposed, either by means of a multi-scale framework [Kourepinis *et al.* (2010); Sethuraman and Reddy (2008)], or by means of an averaged damage quantity defined at the scale of a REV [Suzuki (2012); Valko and Economides (1994)]. The former methods do not allow tracking a damage variable explicitly, while in the latter, the link between length scales involved in stress intensity factors is not justified.

The goal of this research work is to account for crack-induced anisotropy in a consistent damage model for quasi-brittle geomaterials. Emphasis is put on the physical meaning and thermodynamic consistency of the model, and on related numerical issues. Section 2 reviews the main strategies adopted so far to model anisotropy induced by more than one damage mechanism in geomaterials (mainly: tension, compression and shear damage). Section 3 presents the thermodynamic framework and the main assumptions of the proposed anisotropic damage model. Section 4 presents the results of triaxial compression tests simulated at the integration point.

2. A Critical Review of Anisotropic Damage Models

In geomaterials such as rock and concrete, compression strength typically differs by one order of magnitude from tensile strength. Although damage under isotropic compression was observed in hardened cement paste [Ghabezloo *et al.* (2008)], "compression damage" in geomaterials is in general associated to cracking under a differential stress. Let us consider a brittle material sample subjected to a triaxial compression stress (Fig. 1). If the sample is homogeneous and if there is no friction at the top and bottom boundaries, the sample undergoes lateral expansion (Fig. 1(a)).

If boundaries are frictional and the sample is homogeneous, shear cracks will form (Fig. 1(b)). The granular fabric of rock and concrete tends to drive cracks around the stiffest crystals or aggregates, which results in "splitting effects" in tension and "crossing effects" in compression [Ortiz (1985)] (Fig. 2(b)-2(a)). In CDM, crossing effects in geomaterials are most often modeled as tension damage: a crack parallel to the axis, driven by axial compression is considered to have the same mechanical effects as a crack parallel to the axis, driven by lateral tension.

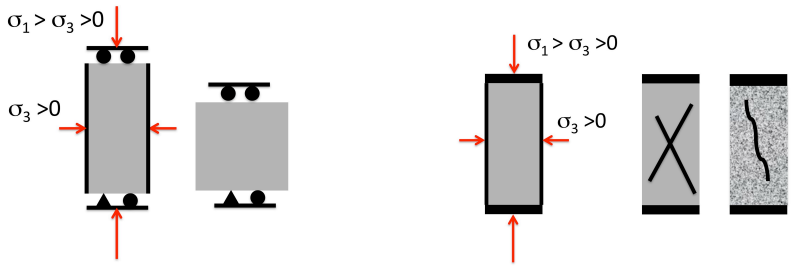

(a) Non Frictional Boundaries (b) Frictional Boundaries

Fig. 1. Expected Crack Path During a Triaxial Compression Test (soil mechanics convention, compression counted positive): (a) non frictional boundaries ; (b) frictional boundaries for a homogeneous material (left) and a granular material (right)

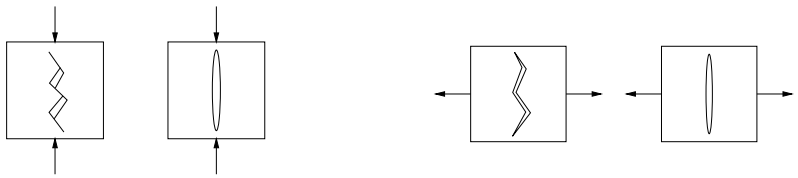

(a) Crossing Effects (b) Splitting Effects

Fig. 2. Schematic representation of crossing (a) and splitting (b) mechanisms.

2.1. *Tension and Compression Damage with Scalar Variables*

CDM initially aimed to model brittle behavior observed in metals [Krajcinovic (1996); Lemaitre and Desmorat (2005)]. In early damage models proposed for concrete [Mazars (1986); Mazars and Pijaudier-Cabot (1989)], two damage scalar variables were introduced in order to distinguish stiffness degradation rates in tension and compression. Following the same idea, Frémond and Nedjar [1996] split the damaged elastic deformation energy into potentials associated to tension and compression. Damage evolution laws are made dependent on negative and positive strains, for compression and tension, respectively.

The formulation proposed by Frémond and Nedjar allows modeling unilateral effects of crack closure on stiffness, i.e. recovery of compression strength without recovery of tension strength when cracks close. Note that damage models resorting to two different scalar variables are weakly anisotropic models: determination of the principal directions of the strain (or stress) tensor is necessary to evaluate the energy

dissipated in tension and in compression. However the scalar form adopted for the damage variables does not allow predicting damage-induced anisotropy: anisotropy of strain (or stress) controls damage rates, but stiffness anisotropy does not depend on damage.

Material softening after the failure peak is known to induce localization effects. In quasi-static problems, ellipticity of the governing equations is lost, while dynamic hyperbolic equations become elliptic [Lasry and Belytschko (1988)]. Energy dissipated by opening new crack surfaces tends to zero, non-elastic deformation localizes at a few integration points, and Finite Element solutions are mesh-dependent. In order to account for the influence of damage defined at $\mathbf{x}$ at location $\mathbf{x} + d\mathbf{x}$, an internal length parameter needs to be introduced in the formulation. Regularization techniques include (i) microstructure-enriched models [Mindlin (1964); Germain (1973a); Germain (1973b); Vardoulakis and Sulem (1995)], (ii) integral and differential non-local formulations [Bazant (1991); Bazant and Jirasek (2002); Jirasek (1998)], (iii) viscoplastic models [Belytschko and Kulkarni (1990)]. Frémond and Nedjar [1996] proposed a gradient-enhanced damage model, in which damage gradients ($\nabla\beta_c$, $\nabla\beta_t$) are part of the internal variables.

In Lubliner's concrete damage model [Lubliner *et al.* (1989)], the damage variable is defined as the ratio of dissipated plastic energy for both tensile and compressive cases. Based on this framework, Lee and Fenves [1998] coupled damage and plasticity by using different hardening variables for different stress states. Damage models that are not coupled to plasticity require the definition of damage potentials. Abu Al-Rub and Kim [2010] used two separate potentials for two different damage variables (damage due to tensile stress, damage due to compressive stress). In Frémond and Nedjar's model [1996], the variables that are work-conjugate to damage variables (called "affinities" or "energy release rates") are discontinuous functions of strain: $\partial\Psi_s/\partial\beta_c$ depends on ϵ^-, and $\partial\Psi_s/\partial\beta_t$ depends on ϵ^+. This implies that the rate of damage depends on a non-differentiable field function, which needs special handling in a numerical code. In Θ-Stock Finite Element code for instance [Gatmiri and Arson (2008)], the damage model assumes an associate flow rule for damage (noted $\mathbf{D}$), in which the damage criterion ($f_d(\mathbf{Y}^+, \mathbf{D})$) is a homogeneous function of degree one in $\mathbf{Y}^+$, and in which the positive part of the energy release rate, $\mathbf{Y}^+$, is proportional to positive deformation: $\mathbf{Y}^+ = g\epsilon^+$. Computation of the increment of damage at iteration i of load step k ($d\mathbf{D}_{(k,i)}$) requires dynamic storage of $\mathbf{Y}^+$ at iterations i and $i-1$:

$$d\mathbf{D} = \dot{\lambda}_d \frac{\partial f_d(\mathbf{Y}^+,\mathbf{D})}{\partial \mathbf{Y}^+} \quad \text{parallel to} \quad d\mathbf{Y}^+$$

$$\left[d\mathbf{Y}^+\right]_{(k,i)} = g\left[d\epsilon^+\right]_{(k,i)} = g\left(\left[\epsilon^+\right]_{(k,i)} - \left[\epsilon^+\right]_{(k,i-1)}\right) = g\left(\left[\mathbf{Y}^+\right]_{(k,i)} - \left[\mathbf{Y}^+\right]_{(k,i-1)}\right) \tag{1}$$

in which $\dot{\lambda}_d$ is the damage multiplier. Moreover, Frémond and Nedjar assume that damage in compression actually produces tension damage - but that the reverse is not true. The elastic domain is defined as:

$$(\beta_t, \beta_c) \in C = \{(x, y), x \in [0, 1]; y \in [0, 1], x \leq y\} \tag{2}$$

The rate of damage (computed from the normality rule) is not unique at singularity points, which raises important numerical issues.

2.2. *Splitting and Crossing Effects with One Tensor Variable*

Anisotropic damage models derive naturally from damage models formulated with a compression damage scalar and a tension damage scalar. In geomechanics, the anisotropic damage variable is usually a second-order tensor which can be viewed as Kachanov's crack density tensor [1992]:

$$\mathbf{D} = \sum_{k=1}^{N} d_k \mathbf{n}_k \otimes \mathbf{n}_k \tag{3}$$

(in which the REV is assumed to contain N cracks characterized by a normal direction $\mathbf{n}_k$ and a volumetric fraction d_k), or as Oda's fabric tensor [1984]:

$$\mathbf{F} = \frac{1}{V_{REV}} \int_0^{\infty} \int_{\Omega} E\left(r, \mathbf{n}\right) d\mathbf{n}\, dr \tag{4}$$

(in which $E\left(r, \mathbf{n}\right)$ is the mathematical expectancy of a crack of radius r and normal direction $\mathbf{n}$ in the REV V_{REV}). For instance, Abu Al-Rub and Kim [2010] and Cicekli *et al.* [2007] used a second-order damage tensor in a free energy potential expressed in terms of elastic strains, while Murakami and Kamiya [1996] adopted the same approach with a different free energy expressed in terms of elastic strain and modified strains. However elastic strains cannot be controlled in an experiment, or imposed as a boundary condition in a numerical code. Therefore Halm and Dragon [1998] and Homand-Etienne *et al.* [1998] expressed rock skeleton free energy in terms of total strains. Chaboche [1993] and Pellet *et al.* [2005] employed a similar strategy, with the additional use of a parameter accounting for non-orthotropic damage. Shao *et al.* 2005; 2006, Zhou *et al.* [2006] and Hayakawa and Murakami [1997] proposed anisotropic damage models based on a stress-dependent free energy potential.

The main limitations of anisotropic damage models used in geomechanics are:
(1) *The difficult expression of a flow rule for anisotropic damage.* As illustrated in Fig. 2(a)-2(b), damage is modeled as tensile cracks, even under (differential) compression stress. Consequently, the damage criterion is generally not expressed in terms of the energy release rate (noted $\mathbf{Y}$) thermodynamically conjugate to damage, but rather in terms of a projection of this energy release rate in the space of positive deformation or positive stress (noted $\mathbf{Y}^+$). As a result, damage evolution law is generally not a true associate flow rule. The damage function is usually expressed in the following form:

$$f_d(\mathbf{Y}^+, \mathbf{D}) = \sqrt{\frac{1}{2}\mathbf{Y}^+ : \mathbf{Y}^+} - C_0 - C_1 Tr\left(\mathbf{D}\right) \tag{5}$$

in which C_0 is the initial damage threshold and C_1 is a material parameter controlling the rate of damage according to the accumulated damage. Based on the flow rule expressed in Eq. 1, Eq. 5 gives a smooth "damage surface" in the space of $\mathbf{Y}^+$ components (octant of a sphere), but a non-smooth surface in the space of $\mathbf{Y}$ (with edges). In general, models that split tensile and compressive strains ([Murakami and Kamiya (1996)]) or stresses ([Abu Al-Rub and Kim (2010); Cicekli *et al.* (2007);

Hayakawa and Murakami (1997)]), exhibit a non-smooth damage surface (in general, several branches with sharp connections).
(2) *The difficult account for possible damage rotation.* Shear induced by crack opening and closure affect material stiffness and make it difficult to ensure thermodynamic consistency [Chaboche (1992)]. Shear rotates the principal bases of stress and strain, which would require updating the principal base of damage at each iteration. To simplify, anisotropic CDM models generally assume that the principal directions of damage correspond to the principal directions of stress or strain. Most anisotropic models are orthotropic. This allows studying planar and cylindrical transverse isotropic configurations - usually, with no rotation of damage directions.

2.3. *Shear Damage Models*

Mixed mode crack propagation is a long-standing problem of fatigue modeling in metals [Irawan *et al.* (2006)]. In rock, the transition from tensile failure (mode I) to shear failure (mode II) is generally modeled by combining Griffith criterion or the modified Griffith criterion (depending on the Unconfined Compressive Strength (UCS)) with Mohr-Coulomb failure criterion [Guéguen and Palciauskas (1994); Goodman (1989)]. Most models accounting for "shear damage" depend on deviatoric stress - not on shear stress - which actually represents differential stress. In general, two damage potentials governing two different damage variables are introduced: one potential controls isotropic damage under the influence of mean stress, and the other controls "shear damage " under the influence of deviatoric stress. Of particular interest is the series of models proposed for salt rock [Chan *et al.* (1998)]. Because deformation induced by dislocation creep is isochoric, crack damage in salt has often been associated to inelastic dilatant deformation. Damage grows in stress states above the "dilatancy boundary", whereas below this boundary, inelastic contractant strains compensate damage deformation [Hou (2003); Lux and Eberth (2007)]. Within the dilatancy boundary, damage cannot grow nor decrease [Hunsche and Hampel (1999)].

Microscopic mechanisms explaining crack initiation under compression were studied by [Ashby and Sammis (1990)]. Locally, axial and radial stresses initiate wing cracks at the tips of inclined flaws (wedge opening), whereas stress concentrations around holes initiate tensile cracks. Both types cracks can be predicted by expressing Stress Intensity Factors (SIFs). A damage model considering the influence of pure shear stress was proposed by Fouinneteau and Pickett [2007] and Shahid and Chang [1995]: the damage variable is used to account for the reduction of shear modulus in laminated composite materials. Other models were proposed to predict shear failure in pure ductile materials - for instance, the modified Gurson model, which is based on micro mechanics. The micro-mechanical model presented in [Tvergaard and Nielsen (2010)], accounts for: (1) the growth of existing voids due to plastic incompressibility, (2) void nucleation, and (3) void softening during shear mechanisms. However, the effect of damage on elastic properties is not captured.

3. A New Model Distinguishing Tension and Compression Damage Induced by Differential Stress

Capturing the difference of resistance of geomaterials in tension and compression is still an open issue in CDM, mainly because the crack representation assumes an equivalence between a crack opening in pure tension ("splitting effects", Fig. 2(b)) and a crack opening in compression under differential stress conditions ("crossing effects", Fig. 2(a)). The model presented in the following aims to overcome this limitation. The framework compromises between physical meaning of damage, thermodynamic consistency requirements, and related numerical issues.

3.1. *Thermodynamic Framework*

Following the framework of hyper-elasticity [Houlsby and Puzrin (2006)], we have :

$$\boldsymbol{\sigma} = \frac{\partial \psi_s}{\partial \boldsymbol{\epsilon}^E} = \mathbb{C}_e(\mathbf{D}) : \boldsymbol{\epsilon}^E; \quad \mathbf{Y} = -\frac{\partial \psi_s}{\partial \mathbf{D}} \tag{6}$$

where ψ_s is the Helmholtz free energy of the solid skeleton; $\mathbb{C}_e$ is the damaged elastic stiffness tensor, depending on the current damage variable $\mathbf{D}$; $\mathbf{Y}$ is the damage driving force; $\boldsymbol{\epsilon}^E$ is the total elastic deformation. Classical CDM models usually assume that the free energy of the skeleton is equal to the damaged elastic deformation energy [Lemaitre and Desmorat (2005)]. It is proposed instead to account for residual crack openings induced by damage [Abu Al-Rub and Voyiadjis (2003)]:

$$\boldsymbol{\epsilon} = \boldsymbol{\epsilon}^{el} + \boldsymbol{\epsilon}^{ed} + \boldsymbol{\epsilon}^{id} = \boldsymbol{\epsilon}^E + \boldsymbol{\epsilon}^{id} \tag{7}$$

in which $\boldsymbol{\epsilon}^{el}$ is the purely elastic deformation, $\boldsymbol{\epsilon}^{ed}$ is the elastic damage-induced deformation due to the degradation of mechanical stiffness, and $\boldsymbol{\epsilon}^{id}$ is the irreversible deformation tensor. This boils down to adding an energy potential to the damaged elastic deformation in the expression of free energy, in order to account for the mechanical work needed to close cracks that remain open after unloading [Arson and Gatmiri (2012); Swoboda and Yang (1999)]. As explained in [Collins and Houlsby (1997); Houlsby and Puzrin (2006)], three functionals are needed to close the model formulation: (1) *the skeleton Helmholtz free energy* Ψ_s (Eq. 6), (2) *a damage criterion* f_d (Eq. 5), and (3) *a dissipation potential* g_d (to derive the evolution laws of internal variables considered in the model). In the most general case, Helmholtz free energy depends on state variables (in the present case: $\boldsymbol{\epsilon}^E$, or its conjugate: $\boldsymbol{\sigma}$) and internal variables ($\mathbf{D}$ and possibly, hardening variables). Dissipation (Φ_s) is assumed to depend on inelastic strains and damage only [Hansen and Schreyer (1994); Houlsby and Puzrin (2006); Yu (2006)]:

$$\Phi_s = \boldsymbol{\sigma} : \dot{\boldsymbol{\epsilon}}^{id} + \mathbf{Y} : \dot{\mathbf{D}} \geq 0 \tag{8}$$

The equation above is valid when there is no hardening, or when hardening depends on the history of damage (in the latter case, inelastic strains and damage are used as hardening variables). To satisfy inequality 8, it is sufficient to ensure separately:

$$\boldsymbol{\sigma} : \dot{\boldsymbol{\epsilon}}^{id} \geq 0, \qquad \mathbf{Y} : \dot{\mathbf{D}} \geq 0 \tag{9}$$

3.2. *Postulate 1: Expression of the Free Energy*

Most anisotropic damage models for geomaterials postulate a skeleton free energy expressed in terms of deformation. As a result, the energy release rate $\mathbf{Y}$ conjugate to damage (also called damage driving force) is also a function of deformation. In order to capture cracks due to "splitting effects" (Fig. 2(b)) and equivalent cracks due to "crossing effects" (Fig. 2(a)), it is necessary to make the damage criterion depend on a tensile damage driving force (Eq. 5 for instance). The damage rate is thus defined as:

$$\dot{\mathbf{D}} = \dot{\lambda}_d \frac{\partial g_d}{\partial \mathbf{Y}^+} \neq \dot{\lambda}_d \frac{\partial g_d}{\partial \mathbf{Y}} \tag{10}$$

which poses two main problems:

(1) The damage flow rule does not fit into the standard thermodynamic framework, in which the rate of an internal variable is proportional to the derivative of a potential by its conjugate driving force.
(2) The damage flow rule expressed in Eq. 10 depends on the derivatives of absolute values, which brings some numerical issues (see Eq. 1 for instance).

In order to better account for states of tensile deformation under differential stress, the free energy potential is expressed in terms of stress (Gibbs free energy, G_s). To stay within the framework of linear elasticity in the absence of damage, the expression of the free energy should have at most quadratic terms in $\boldsymbol{\sigma}$ [Halm and Dragon (1998); Shao *et al.* (2005)]. In addition, it is assumed that G_s is linear in $\mathbf{D}$, according to the expression proposed by Shao *et al.* [2005]:

$$\begin{aligned} G_s\left(\boldsymbol{\sigma}, \mathbf{D}\right) = \frac{1}{2}\boldsymbol{\sigma} : \mathbb{S}_0 : \boldsymbol{\sigma} + a_1 \mathrm{tr}\mathbf{D}\left(\mathrm{tr}\boldsymbol{\sigma}\right)^2 + a_2 \mathrm{tr}(\boldsymbol{\sigma}\cdot\boldsymbol{\sigma}\cdot\mathbf{D}) \\ + a_3 \mathrm{tr}\boldsymbol{\sigma}\,\mathrm{tr}(\mathbf{D}\cdot\boldsymbol{\sigma}) + a_4 \mathrm{tr}\mathbf{D}\,\mathrm{tr}(\boldsymbol{\sigma}\cdot\boldsymbol{\sigma}) \end{aligned} \tag{11}$$

in which $\mathbb{S}_0$ is the compliance of the intact material, in the absence of damage. Note that this expression of G_s can actually be obtained from the expression of Ψ_s chosen by Halm and Dragon [1998] through a Legendre transform:

$$\psi_s\left(\boldsymbol{\epsilon}^E, \mathbf{D}\right) + G_s\left(\boldsymbol{\sigma}, \mathbf{D}\right) = \boldsymbol{\sigma} : \boldsymbol{\epsilon}^E \tag{12}$$

The material parameters a_i need to be calibrated by numerical simulation [Shao *et al.* (2005)]. According to Eq. 11, the stress/strain relationship writes:

$$\begin{aligned} \boldsymbol{\epsilon}^E = \boldsymbol{\epsilon} - \boldsymbol{\epsilon}^{id}(\mathbf{D}) = \frac{\partial G_s}{\partial \boldsymbol{\sigma}} = \frac{1+\nu_0}{E_0}\boldsymbol{\sigma} - \frac{\nu_0}{E_0}(\mathrm{tr}\boldsymbol{\sigma})\,\boldsymbol{\delta} + 2a_1(\mathrm{tr}\mathbf{D}\,\mathrm{tr}\boldsymbol{\sigma})\,\boldsymbol{\delta} \\ + a_2(\boldsymbol{\sigma}\cdot\mathbf{D} + \mathbf{D}\cdot\boldsymbol{\sigma}) + a_3[\,\mathrm{tr}(\boldsymbol{\sigma}\cdot\mathbf{D})\,\boldsymbol{\delta} + (\mathrm{tr}\boldsymbol{\sigma})\,\mathbf{D}\,] + 2a_4(\mathrm{tr}\mathbf{D})\,\boldsymbol{\sigma} \end{aligned} \tag{13}$$

where $\boldsymbol{\delta}$ is the second-order identity tensor, and E_0 and ν_0 are Young's modulus and Poisson's ratio of the intact material. Similarly the damage driving force writes:

$$\mathbf{Y} = -\frac{\partial \psi_s}{\partial \mathbf{D}} = \frac{\partial G_s}{\partial \mathbf{D}} = a_1(\mathrm{tr}\boldsymbol{\sigma})^2\,\boldsymbol{\delta} + a_2\boldsymbol{\sigma}\cdot\boldsymbol{\sigma} + a_3\mathrm{tr}(\boldsymbol{\sigma})\boldsymbol{\sigma} + a_4\mathrm{tr}(\boldsymbol{\sigma}\cdot\boldsymbol{\sigma})\boldsymbol{\delta} \tag{14}$$

3.3. *Postulate 2: Damage Function*

3.3.1. *Original Drucker-Prager Yield Surface*

Drucker-Prager model is a plasticity model capturing "crossing effects" under differential stress and accounting for the difference of material behavior when the material is overall in tension or overall in compression. Drucker-Prager yield function writes:

$$f(\boldsymbol{\sigma}) = \sqrt{J_2} - \alpha I_1 - k \tag{15}$$

in which I_1 and J_2 are the first and second stress invariants, respectively. Material parameters are given as:

$$\alpha = \frac{2\sin\phi}{\sqrt{3}(3-\sin\phi)}, \quad k = \frac{6c\cos\phi}{\sqrt{3}(3-\sin\phi)} \tag{16}$$

where ϕ is the angle of internal friction, and c is cohesion. Figure 3(a) shows the yield surface in 3-D space with $\phi = 20°$, $c = 2\,kPa$. Note that in this figure, the soil mechanics sign convention is adopted, i.e. compression is counted positive, and tension is counted negative. A natural choice would be to use the first and second invariants of the damage driving force $\mathbf{Y}$ instead of I_1 and J_2 in Eq. 15, in order to obtain the damage criterion. The damage surface in $\mathbf{Y}$ space would be the same as the yield surface plotted in stress space for plasticity. But Fig. 3(b) shows that for the choice of free energy in Eq. 11, the corresponding damage surface in stress space would have symmetries implying that damage thresholds are the same in tension and in compression. This is not satisfactory for geomaterials. To overcome this problem, one possibility is to change the expression of the free energy in order to avoid having a damage driving force depend only on quadratic stress terms (Eq. 14). However, it is not desirable, because the polynomial expression of G_s in (Eq. 11) is in part dictated by elasticity requirements (for the terms in $\boldsymbol{\sigma}$), and in part verified by experiments (for the terms in $\mathbf{D}$). It is proposed instead to adapt the expression of the damage function to distinguish compression and tension strengths.

3.3.2. *Modified Damage Surface*

The modified expression of the damage function is written in the following form:

$$f_d = \sqrt{J^*} - \alpha I^* - k \tag{17}$$

J^* and I^* are defined as:

$$J^* = \frac{1}{2}(\mathbb{P}_1 : \mathbf{Y} - \frac{1}{3}I^*\boldsymbol{\delta}) : (\mathbb{P}_1 : \mathbf{Y} - \frac{1}{3}I^*\boldsymbol{\delta}), \quad I^* = (\mathbb{P}_1 : \mathbf{Y}) : \boldsymbol{\delta} \tag{18}$$

in which $\mathbb{P}_1$ is a fourth-order projection tensor defined as:

$$\mathbb{P}_1(\boldsymbol{\sigma}) = \sum_{p=1}^{3} \left[H(\sigma^{(p)}) - H(-\sigma^{(p)})\right] \mathbf{n}^{(p)} \otimes \mathbf{n}^{(p)} \otimes \mathbf{n}^{(p)} \otimes \mathbf{n}^{(p)} \tag{19}$$

in which $H(\cdot)$ is the Heaviside distribution function, $\sigma^{(p)}$ is the p^{th} eigenstress value, and $\mathbf{n}^{(p)}$ is the vector alined with the p^{th} principal direction of stress. α is a material

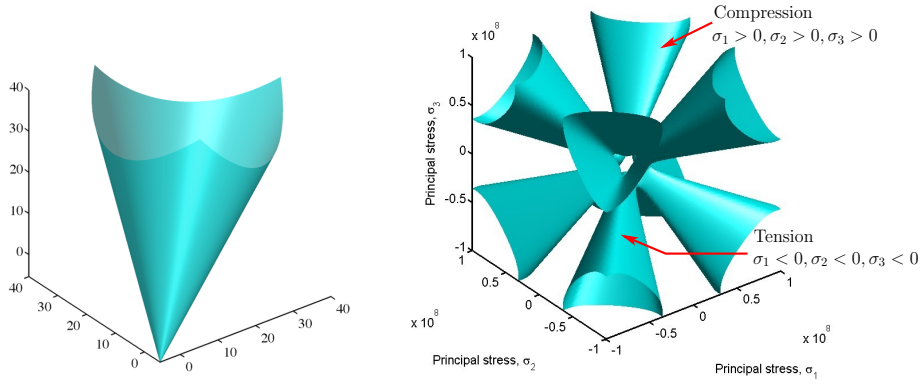

(a) Drucker-Prager yield surface. (b) Drucker-Prager Model in Damage Mechanics.

Fig. 3. For the chosen expression of free energy G_s, replacing stress by damage driving force in Drucker-Prager 's yield function does not define a satisfactory damage surface: damage thresholds are the same in tension and in compression.

parameter accounting for the aperture of the cone in the $\mathbb{P}_1 : \mathbf{Y}$ space. The threshold k in Eq. 17 is defined as a linear function of damage (similar to Eq. 5), suitable for rock [Homand-Etienne *et al.* (1998); Shao *et al.* (2005); Shao *et al.* (2006)]:

$$k = C_0 - C_1 Tr\,(\mathbf{D}) \tag{20}$$

Note that in the preceding equations, the soil mechanics sign convention is adopted (compression positive, tension negative). The projection tensor $\mathbb{P}_1$ ensures that the occurrence of damage be controlled by the action of the damage driving force in the stress principal directions, and that in each stress principal direction, the eigenvalues of the "physical damage driving force tensor" $(\mathbb{P}_1 : \mathbf{Y})$ be of the same sign as the stress eigenvalues. In $\mathbb{P}_1 : \mathbf{Y}$ space, the damage surface is a cone - similar to Drucker-Prager yield surface. The plots of the damage surface (Fig. 4-5), show that the damage surface is locally convex but globally non convex. Note that surface convexity is a sufficient but not necessary condition to satisfy the positivity of the dissipation potential [Desmorat (2006)]: the thermodynamic framework is indeed consistent as long as the damage rate is non-negative. In fact the sign of energy dissipation is only load path dependent, i.e. it should only be *locally* positive. If the surface is locally non-convex, the load path may cross the damage surface, and the predicted state of stress may fall outside the damage surface. Numerical solutions were proposed in [Carstensen *et al.* (2002); Pedroso *et al.* (2008)].

In elasto-plasticity, an associate flow rule based on Drucker-Prager yield function allows accounting for plastic dilatant volumetric strains due to mean stress. The term αI_1 in Eq. 15 is used to account for dilatant effects. The damage rates obtained from an associate flow rule (with the damage function defined in Eq. 17) are not detailed here, for the sake of brevity. It can be shown that the term αI^* may cause

the damage rate to be negative. For instance, Fig. 6 shows that some components of the rate of a dissipation variable computed from an associate flow rule can be negative, depending on the location of the state of stress on the yield surface. To ensure the positivity of dissipation, it is proposed resort to a non-associate flow rule, i.e. to introduce a damage potential $g_d \neq f_d$ in the formulation.

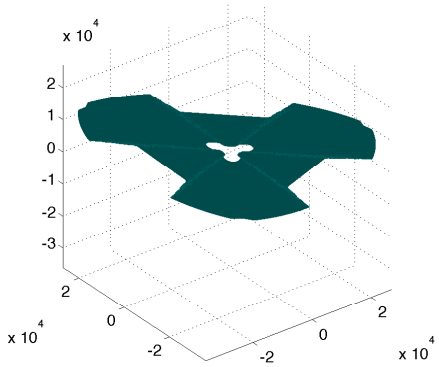

Fig. 4. Damage surface in $\mathbf{Y}$ space.

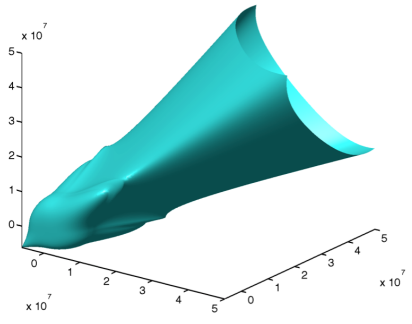

Fig. 5. Damage surface in $\boldsymbol{\sigma}$ space.

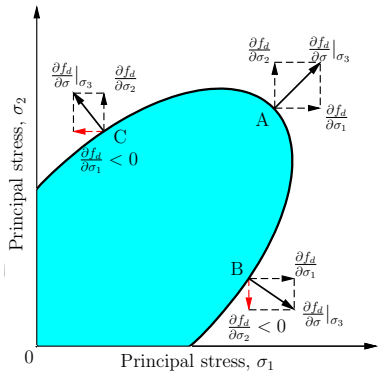

Fig. 6. With an associate flow rule, some components of the rate of damage are negative.

3.4. *Postulate 3: Expression of the Damage Potential*

It is proposed to define the damage potential as a homogeneous function of degree one in $\mathbf{Y}$ [Senseny *et al.* (1992); Collins and Houlsby (1997)]:

$$g_d = \sqrt{\frac{1}{2}(\mathbb{P}_2 : \mathbf{Y}) : (\mathbb{P}_2 : \mathbf{Y})} - C_2 \tag{21}$$

The projection tensor $\mathbb{P}_2$ is introduced to represent both "crossing" and "splitting" effects (Fig. 2(a)-2(b)):

$$\mathbb{P}_2 = \sum_{p=1}^{3} H\left[\max_{q=1}^{3}(\sigma^{(q)}) - \sigma^{(p)}\right] \mathbf{n}^{(p)} \otimes \mathbf{n}^{(p)} \otimes \mathbf{n}^{(p)} \otimes \mathbf{n}^{(p)} \tag{22}$$

Due to the definition of the projection tensor $\mathbb{P}_2$, the surface of the dissipation potential in the space of the components of $\mathbf{Y}$ exhibits three "branches", corresponding to the three possible directions of maximum eigenstress (these three "branches" are plotted with three different colors in Fig. 7). When the maximum eigenstress changes from one direction to another, the state of stress represented by the thermodynamic damage driving force jumps from one "branch" (or subsurface) to another. For the special case when two eigenstresses are equal, the plot of the damage potential exhibits a discontinuity, and the state of stress is characterized by a plane or a line. That could pose numerical problems if there was no unique way to compute the derivative of the damage potential. But in fact, a close form solution exists (not detailed here for the sake of brevity). As a result, the model is thermodynamically consistent and the incremental equations can be implemented in a numerical code. Computations of damage for basic loading paths show that with the dissipation potential defined in Eq. 21, it is possible to calibrate the material parameters a_i in order to ensure the positivity of the components of $\frac{\partial g_d}{\partial \mathbf{Y}}$ (for the sake of brevity, the detailed computations are not provided in this paper). Positivity of $\frac{\partial g_d}{\partial \mathbf{Y}}$ ensures the positivity of the damage rate, and therefore, the thermodynamic consistency of the model. Note that in the space of the "physical damage driving force" $\mathbb{P}_2 : \mathbf{Y}$, the surface of the damage potential is an octant of a sphere (Fig. 8). Fig. 9 shows the shape of the damage potential in the space of stress: the three "branches" have the shape of cones. The three planes departing from the cone intersections illustrate the states of stress for which two maximum eigenstresses have the same value.

3.5. *Postulate 4: Irreversible Deformation Flow Rule*

As explained above (Eq. 9), a sufficient condition to ensure the positivity of dissipation is to ensure that $\mathbf{Y} : \dot{\mathbf{D}} \geq 0$ and $\boldsymbol{\sigma} : \dot{\boldsymbol{\epsilon}}^{id} \geq 0$. According the preceding computations, the condition $\mathbf{Y} : \dot{\mathbf{D}} \geq 0$ is ensured by calibrating the material parameters (a_i) in such a way that the damage rate remains positive for the states of stress expected in geomechanical problems (mainly: trixial and uniaxial compression, and uniaxial tension). A logical choice would be to use the same potential as for damage. The non-associate flow rule would write:

$$\dot{\boldsymbol{\epsilon}}^{id} = \dot{\lambda}_d \frac{\partial g_d}{\partial \boldsymbol{\sigma}} = \dot{\lambda}_d \frac{\partial g_d}{\partial \mathbf{Y}} \frac{\partial \mathbf{Y}}{\partial \boldsymbol{\sigma}} = \dot{\mathbf{D}} \frac{\partial \mathbf{Y}}{\partial \boldsymbol{\sigma}} \tag{23}$$

The flow of irreversible strain should be normal to the surface of the plot shown in Fig. 9. A quick glance at the plot shows that the principal directions of the irreversible strain rate are equal to the stress principal directions, and that in each principal direction, the rate of irreversible strains has the same sign as the stress

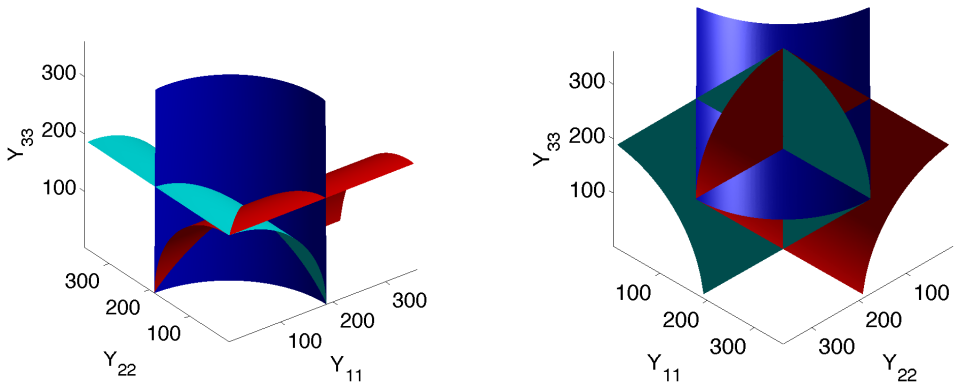

Fig. 7. Damage potential in $\mathbf{Y}$ space. For a given state of stress, the elastic domain is delimited by one of the three colored surfaces (the red (respectively blue and turquoise) surface corresponds to a stress state in which $\sigma^{(1)}$ (respectively $\sigma^{(2)}$ and $\sigma^{(3)}$) is maximum. The figure on the right shows the convex elastic domain common to all possible states of stress.

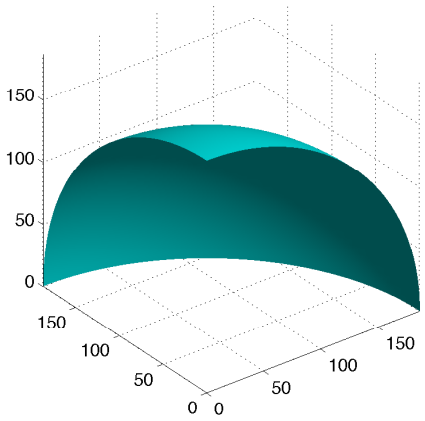

Fig. 8. Damage surface in $\mathbb{P}_2 : \mathbf{Y}$ space.

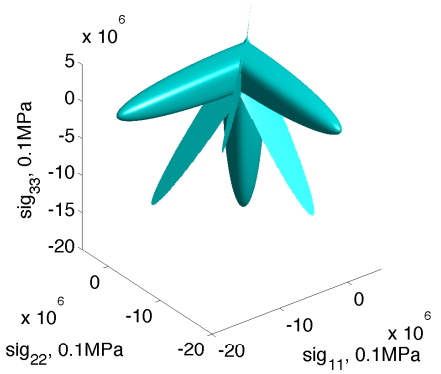

Fig. 9. Damage potential in $\boldsymbol{\sigma}$ space.

rate. However, it is assumed (from Postulate 3) that damage propagates in planes normal to the major principal stress direction, i.e. that cracks opening due to a compression in direction 1 should induce dilatant irreversible deformation in directions 2 and 3. As a result, we cannot reasonably assume that the rate of strain should be parallel and of the same sign as the rate of stress. Instead of deriving the rate of irreversible deformation from the potential (Eq. 21), the evolution law

of irreversible strain is derived from an associate flow rule:

$$\dot{\boldsymbol{\epsilon}}^{id} = \dot{\lambda}_d \frac{\partial f_d}{\partial \boldsymbol{\sigma}} = \dot{\lambda}_d \frac{\partial f_d}{\partial \mathbf{Y}} \frac{\partial \mathbf{Y}}{\partial \boldsymbol{\sigma}} \tag{24}$$

With:

$$\begin{aligned} &\frac{\partial f_d}{\partial \mathbf{D}} = -C_1 \boldsymbol{\delta}; \quad \frac{\partial g}{\partial \mathbf{Y}} = \frac{(\mathbb{P}_2 : \mathbf{Y}) : \mathbb{P}_2}{\sqrt{2(\mathbb{P}_2 : \mathbf{Y}) : (\mathbb{P}_2 : \mathbf{Y})}} \\ &\frac{\partial f_d}{\partial \mathbf{Y}} = \frac{\left[\mathbb{P}_1 : \mathbf{Y} - \frac{1}{3}(\boldsymbol{\delta} : \mathbb{P}_1 : \mathbf{Y})\boldsymbol{\delta}\right] : \left[\mathbb{P}_1 - \frac{1}{3}\boldsymbol{\delta} \otimes (\boldsymbol{\delta} : \mathbb{P}_1)\right]}{\sqrt{2\left[\mathbb{P}_1 : \mathbf{Y} - \frac{1}{3}(\boldsymbol{\delta} : \mathbb{P}_1 : \mathbf{Y})\boldsymbol{\delta}\right]\left[\mathbb{P}_1 : \mathbf{Y} - \frac{1}{3}(\boldsymbol{\delta} : \mathbb{P}_1 : \mathbf{Y})\boldsymbol{\delta}\right]}} - \alpha \boldsymbol{\delta} : \mathbb{P}_1 \end{aligned} \tag{25}$$

4. Simulation of Anisotropic Damage During Triaxial Compression

The model presented in Section 3 was implemented in a program computing stress and damage at the integration point. The values of material parameters (in Tab. 1) are taken from [Shao *et al.* (2006)]. Note that these values were calibrated for granite rock with the damage model presented in [Shao *et al.* (2006)]. The damage model proposed herein is different, so the simulation results are not expected to represent the behavior of granite rock.

Table 1. Parameters Used in the Simulations with the Proposed Damage Model.

E_0 GPa	ν_0	a_1 $\times 10^{-4}$GPa^{-1}	a_2 $\times 10^{-4}$GPa^{-1}	a_3 $\times 10^{-4}$GPa^{-1}	a_4 $\times 10^{-4}$GPa^{-1}	α	C_0 MPa
68	0.21	1.2565	393.71	-12.565	2.513	0.2309	0.001

In the triaxial compression test is presented in Fig. 10-11, the first loading stage (OA) consists in imposing an isotropic confining pressure of 10MPa. In a second stage, strain in direction 1 is increased by increments (positive with the soil mechanics sign convention, up to 0.75%), while stress in directions 2 and 3 is maintained constant ($\dot{\sigma}_2 = \dot{\sigma}_3 = 0$). The increae of strain in direction 1 will thus cause an increase of deviatoric stress $\dot{\sigma}_1 - \dot{\sigma}_3 \neq 0$: AB represents the elastic loading path, while BC is the non-elastic loading path (when cracks propagate). The unloading phase (CD), when ϵ_1 is relaxed, is also simulated. It is expected to get damage only in planes perpendicular to directions 2 and 3 ($D_2 = D_3 > 0$), while irreversible strains should be compression deformation in direction 1 ($\epsilon_1^{ir} > 0$) and tension deformation in directions 2 and 3 ($\epsilon_2^{ir} = \epsilon_3^{ir} < 0$). The model predicts indeed that the damaged stiffness of the material is less than the original stiffness (Fig. 10), which proves that damage occurred (Fig. 11). It can also be noticed that relaxing deformation is not sufficient to release the compression stress originated by the strain imposed to the sample during the test. The maximum deviatoric stress during the test is 235 MPa (i.e. a total compression of 245MPa in direction 1). This corresponds to the maximum strain imposed in direction 1 (0.75%). As the strain in direction 1 is increased, cracks in planes perpendicular to directions 2 and 3 propagate (Fig. 11): correspondingly, damage accumulates in directions 2 and 3 (up to $D_2 = D_3 = 65\%$). Then

$D_2 = D_3$ remains constant during the isotropic compression and unloading phases. In fact damage is generated when the lateral surface of the sample is subjected to compression stress, but lateral strains change from compression deformation (OA) to tension deformation (AC) (Fig. 10). No damage occurrs in the vertical direction during the test.

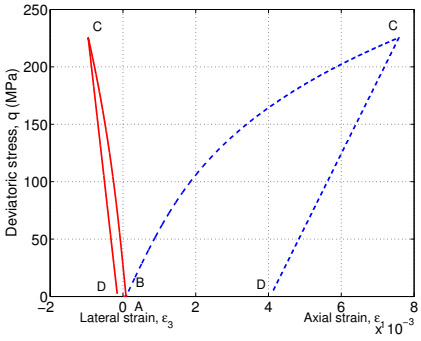

Fig. 10. Triaxial Compression Test. Deviatoric stress versus axial strains.

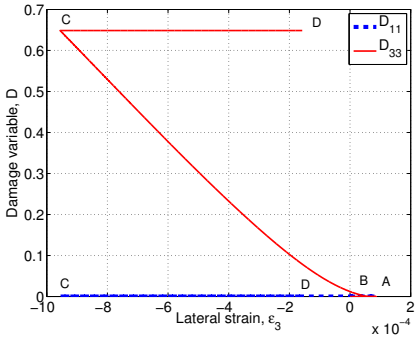

Fig. 11. Triaxial Compression Test. Damage evolution with lateral strain ϵ_3.

Confinement delays the occurrence of damage. Fig. 12 shows that during a strain-controlled triaxial compression test, the damage threshold is reached for a higher deviatoric stress when the confining stress increases. For lower confining stress, damage occurs at a smaller deviatoric stress, the cumulated damage is less, and the lateral residual strain is higher . The simulation results obtained with the parameters suggested by Shao [2006] show that the proposed model captures qualitatively the most important features of damaged rock behavior under differential stress. The values of parameters a_1, a_2, a_3 and a_4 may be adjusted to brittle or ductile responses. A parametric study on a_1 is shown in Fig. 13 for the triaxial compression test under 10 MPa of confining stress (with the values of a_2, a_3 and a_4 reported in Tab. 1). Decreasing the value of parameter a_1 tends to increase lateral expansion due to residual crack openings, which could be appropriate for a more ductile rock.

5. Conclusion

At the scale of the Representative Elementary Volume (REV), Continuum Damage Mechanics (CDM) models for geomaterials assume that cracks propagate in mode I. Both splitting and crossing effects are modeled by a Griffith crack, opening under the influence of a differential stress. This approach allows representing crack-induced orthotropic damage and potential unilateral effects due to crack closure. However, the approach fails at predicting rotation of the principal directions of damage due to

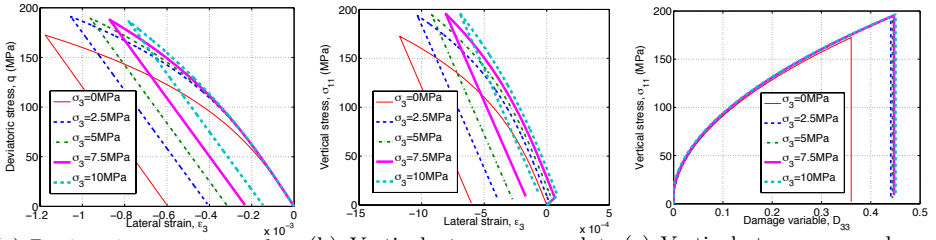

(a) Deviatoric stress versus lateral strain ϵ_3 (set to 0 after applying the confining stress).

(b) Vertical stress versus lateral strain ϵ_3.

(c) Vertical stress versus damage variable D_{33}.

Fig. 12. Triaxial compression Tests with different confining stresses.

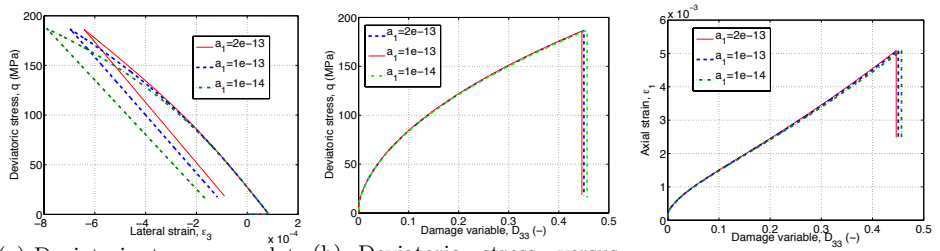

(a) Deviatoric stress versus lateral strain ϵ_3.

(b) Deviatoric stress versus damage variable D_{33}.

(c) Damage evolution with axial strains ϵ_1.

Fig. 13. Triaxial compression Tests with different values of a_1.

shear stress. On the one hand, shear damage models assume several dissipation potentials: one for isotropic damage due to volumetric stress, and one for orthotropic damage due to deviatoric stress. On the other hand, orthotropic damage models often assume that the principal base of damage is the same as stress, and related simulations assume a constant stress principal base. Another recurring limitation of CDM models proposed for geomaterials is the difficulty to account for different damage thresholds in tension and compression when the damage driving force is assumed to be a function of differential stress. A new anisotropic damage model is proposed to overcome these problems.

The formulation compromises between thermodynamic requirements, physical expectations and differentiability requirements for energy potentials. The solid skeleton free energy is a polynomial of order two in stress, and order one in damage. Damage is a second-order tensor. Contrary to existing damage models proposed for geomaterials, flow rules are derived with the energy release rate work-conjugate to damage, which is thermodynamically consistent. The damage criterion is adapted from Drucker-Prager yield function: the criterion is expressed in terms of damage energy release rate, and a projector is used in order to distinguish between tension and compression damage thresholds. Positivity of dissipation is ensured by com-

puting the damage rate by a non-associate flow rule. On the contrary, non-elastic deformation due to damage needs to be computed by the associate flow rule in order to maintain the physical meaning of the model trends.

Triaxial compression tests were simulated at the integration point. The model captures well the propagation of crack planes in the direction parallel to major compression stress, and the subsequent anisotropy induced on stiffness and deformation. In addition, the damage criterion allows to distinguish between crack propagation in tension and compression. More work is needed to calibrate the model parameters, and to determine precisely whether for these calibrated parameters, all states of stress lead to a positive dissipation.

The proposed model is expected to give useful insights for the formulation of new constitutive models for rock and concrete. It is also the first step towards the development of a framework allowing modeling multi-scale crack propagation - without converting one scale of discontinuity into a continuous damaged zone. In particular, further studies will be dedicated to the implementation of anisotropic Continuum Damage Mechanics models into Extended Finite Element programs.

Acknowledgments

This study was conducted at Texas A&M University and at the Georgia Institute of Technology, as part of a research program on Finite Element Modeling of Hydraulic Fracturing. Funding was provided by ConocoPhillips, Houston, Texas.

References

Abu Al-Rub, R.K. and Voyiadjis, G.Z. (2003). On the coupling of anisotropic damage and plasticity models for ductile materials. *Int. J. Solids A/ Struct.*, **40**: 2611–2643.

Abu Al-Rub, R. K. and Kim, S.-M. (2010). Computational applications of a coupled plasticity-damage constitutive model for simulating plain concrete fracture. *Engineering Fracture Mechanics*, **77**: 1577–1603.

Arson, C. and Gatmiri, B. (2012). Thermo-Hydro-Mechanical Modeling of Damage in Unsaturated Porous Media: Theoretical Framework and Numerical Study of the EDZ. *International Journal for Numerical and Analytical Methods in Geomechanics*, **36**: 272–306.

Ashby, M. F. and Sammis, C. G. (1990). The damage mechanics of brittle solids in compression. *Pure and Applied Geophysics*, **133**(3): 489–521.

Bazant, Z. (1991). Why continuum damage is nonlocal : micromechanics arguments. *Journal of Engineering mechanics, ASCE*, **117**(5): 1070–1087.

Bazant, Z. and Jirasek, M. (2002). Nonlocal integral formulations of plasticity and damage: survey of progress. *Journal of Engineering Mechanics, ASCE*, **128**(11): 1119–1149.

Belytschko, T. and Kulkarni, M. (1990). On imperfections and spatial gradient regularization in strain softening viscoplasticity. in: *Failure criteria and analysis in dynamic response*, H.E. Lindberg and Aptek (eds), American Society of Mechanical Engineers, Chap. 107, 1–5.

Carstensen, C., Hackl, K. and Mielke, A. (2002). Non-convex potentials and microstructures in finite-strain plasticity. *Royal Society of London Proceedings Series A*, **458**(2018): 299–317.

Chaboche, J.-L. (1992). Damage Induced Anisotropy: On the Difficulties Associated with the Active/Passive Unilateral Condition. *International Journal of Damage Mechanics*, **1**: 148–171.

Chaboche, J.-L. (1993). Development of continuum damage mechanics for elastic solids sustaining anisotropic and unilateral damage. *International Journal of Damage Mechanics*, **2**: 311–329.

Chan, K. S., Bodner, S. R. and Munson, D. E. (1998). Recovery and healing of damage in WIPP salt. *International Journal of Damage Mechanics*, **7**: 143-166.

Cicekli, U., Voyiadjis, G. Z. and Abu Al-Rub, R. K. (2007). A plasticity and anisotropic damage model for plain concrete. *International Journal of Plasticity*, **23**: 1874–1900.

Collins, I. F. and Houlsby, G. T. (1997). Application of thermomechanical principles to the modelling of geotechnical materials. *Proceedings: Mathematical, Physical and Engineering Sciences*, **453**: 1975–2001.

Desmorat, R. (2006). Positivité de la dissipation intrinsèque d'une classe de modèles d'endommagement anisotropes non standards. *Comptes Rendus Mecanique*, **334**: 587–592.

Dormieux, L., Kondo, D., Ulm, F.-J. (2006). A micro mechanical analysis of damage propagation in fluid-saturated cracked media. *C.R. Mécanique*, **334**: 440–446.

Fouinneteau, M. R. C., and Pickett, A. K. (2007). Shear mechanism modelling of heavy tow braided composites using a meso-mechanical damage model. *Composites Part A: Applied Science and Manufacturing*, **38**: 2294–2306.

Frémond, M. and Nedjar, B. (1996). Damage, gradient of damage and principle of virtual power. *International Journal of Solids and Structures*, **33**: 1083–1103.

Gatmiri, B. and Arson, C. (2008). Theta-Stock, a powerful tool for thermohydromechanical behaviour and damage modelling of unsaturated porous media. *Computers & Geotechnics*, **35**(6): 890–915.

Germain, P. (1973). La méthode des puissances virtuelles en mécanique des milieux continus. Première partie : théorie du second gradient. *J. de Mécanique*, **12**(2):235–274.

Germain, P. (1973). The method of virtual power in continuum mechanics. Part 2: Microstructure. *J. Appl. Math.*, **25**(3): 556–575.

Ghabezloo, S. and Sulem, J. and Guédon, S. and Martineau, F. and Sant-Marc, J. (2008). Poromechanical behavior of hardened cement paste under isotropic loading. *Cement and Concrete Research*, **38**: 1424–1437.

Guéguen, Y. and Palciauskas, V. Introduction to the Physics of Rocks. *Princeton University Press*, 1994.

Guéguen, A.A.-C., Cormery, F., Shao, J.-F., Kondo, D. (2008). A micromechanical model of elastoplastic and damage behavior of a cohesive geomaterial. *International Journal of Solids and Structures*, **45**, 1406–1429.

Goodman, R. E. Introduction to Rock Mechanics. *Wiley; 2nd edition*, 1989.

Halm, D. and Dragon, A. (1998). An anisotropic model of damage and frictional sliding for brittle materials. *Engineering Fracture Mechanics*, **25**: 729–737.

Nansen, N.R. and Schreyer, H.L. (1994). A thermodynamically consistent framework for theories of elastoplasticity coupled with damage. *Int. J. Solids and Structures*, **31**(3): 359–389.

Hayakawa, K. and Murakami, S. (1997). Thermodynamical modeling of elastic-plastic damage and experimental validation of damage potential. *International Journal of Damage Mechanics*, **6**: 333–363.

Homand-Etienne, F. Hoxha, D. and Shao, J. F. (1998). A continuum damage constitutive law for brittle rocks. *Computers and Gotechnics*, **22**: 135–151.

Hou, Z. (2003). Mechanical and hydraulic behavior of rock salt in the excavation disturbed

zone around underground facilities. *International Journal of Rock Mechanics & Mining Sciences*, **40**: 725–738.

Houlsby, G.T. and Puzrin, A.M. (2006). Principles of Hyperplasticity. An Approach to Plasticity Theory Based on Thermodynamic Principles. *Springer*.

Hunsche, U. and Hampel, A. (1999). Rock salt - the mechanical properties of the host rock material for a radioactive waste repository. *Engineering Geology*, **52**: 271–291.

Irawan, Y.S. and Hagiwara, Y. and Ohya, S.I. (2006). Predictions of Anisotropy Affected Fatigue Crack Propagation Paths in Pure Aluminum Sheets. *International Journal of Computational Methods*, **3**(1): 83–96.

Jirasek, M. (1998). Nonlocal models for damage and fracture : comparison of approaches. *Int. J. Solids and Struct.*, **35**(31-32): 4133–4145.

Kachanov, M. (1992). Effective elastic properties of cracked solids: critical review of som basic concepts. *Appl. Mech. Rev.*, **45**(8): 304–335.

Kourepinis, D. and Pearce, C. and Bicanic, N. (2010). Higher-Order Discontinuous Modeling or Fracturing In Concrete Using the Numerical Manifold Method. *International Journal of Computational Methods*, **7**(1): 83–106.

Krajcinovic D. Damage Mechanics. *North-Holland, series in Applied Mathematics and Mechanics, Elsevier*, 1996.

Lasry, D. and Belytschko, T. (1988). Localization limiters in transient problems. *Int. J. Solids and Struct.*, **24**(6): 581–597.

Lee, J. and Fenves, G. (1998). Plastic-damage model for cyclic loading of concrete structures. *Journal of Engineering Mechanics*, **124**: 892–900.

Lemaître A, Desmorat R. Engineering Damage Mechanics. Ductile, creep, fatigue and brittle failure. *Springer - Verlag, Berlin Heidelberg*, 2005.

Li, S. and Ghosh, S. (2004). Debonding in Composite Microstructures with Morphological Variations. *International Journal of Computational Methods*, **1**(1): 121–149.

Loucks, R.G. and Reed, R.M. and Ruppel, S.C. and Jarvie, D.M. (2009). Morphology, Genesis, and Distribution of Nanometer-Scale Pores in Siliceous Mudstones of the Mississippian Barnett Shale. *Journal of Sedimentary Research*, **79**:848–861

Lubliner, J., Oliver, J., Oller, S. and Onate, E. (1989). A plastic-damage model for concrete. *International Journal of Solids and Structures*, **25**: 299–326.

Lux, K.H. and Eberth, S. (2007). Fundamentals and first application of a new healing model for rock salt. *The Mechanical Behavior of Salt - Understanding the THMC Processes in Salt, Wallner, Lux Minkley & Hardy, Jr (eds), Taylor & Francis Group, London*, pp.129–138.

Mazars, J. (1986). A description of micro- and macro scale damage of concrete structures. *J. Eng. Mech.*, **115**: 345–365.

Mazars, J. and Pijaudier-Cabot, G. (1989). Continuum damage theory - application to concrete. *J. Eng. Mech.*, **115**: 345–365.

Mazars, J. and Pijaudier-Cabot, G. (1996). From Damage to Fracture Mechanics and Conversely: A Combined Approach. *International Journal of Solids and Structures*, **33**(22): 3327–3342.

Mindlin, R.D. (1964). Micro-structure in linear elasticity. *Archiv Rational Mech. Anal.*, **16**:51–78.

Murakami, S. and Kamiya, K. (1996). Constitutive and damage evolution equations of elastic-brittle materials based on irreversible thermodynamics. *Int. J. Mech. Sci.*, **39**: 473–486.

Nagashima, T. and Suemasu, H. (2006). Stress analyses of Composite Laminate with Delamination Using X-FEM. *International Journal of Computational Methods*, **3**(4): 521–543.

Oda, M. (1984). Similarity Rules of Crack Geometry in Statistically Homogeneous Rock Masses. *Mech. of Materials*, **3**: 119–129.

Ortiz, M. (1985). A constitutive theory for the inelastic behaviour of concrete. *Mech. of Materials*, **4**: 67–93.

Pedroso, D. M., Sheng, D. and Sloan, S. W. (2008). Stress update algorithm for elastoplastic models with nonconvex yield surfaces. *International Journal for Numerical Methods in Engineering*, **76**: 2029–2062.

Pellet, F., Hajdu, A., Deleruyelle, F. and Besnus, F. (2005). A viscoplastic model including anisotropic damage for the time dependent behaviour of rock. *Int. J. Numer. Anal. Meth. Geomech.*, **29**: 941–970.

Pensée, V., Dormieux, L., Kondo, D. (2002). Micro-mechanical Analysis of Anisotropic Damage in Brittle Materials. *C.R. Journal of Engineering Mechanics*, **128**(8): 889–897.

Senseny, P. E., Hansen, F. D., Russell, J. E., Carter, N. L. and Handin, J. W. (1992). Mechanical behaviour of rock salt: Phenomenology and micromechanisms. *International Journal of Rock Mechanics and Mining Sciences & Geomechanics Abstracts*, **29**: 363–378.

Sethuraman, R. and Reddy, C.S. (2008). Pseudo-Elastic Analysis of Elastic-Plastic Crack Tip Fields Using Element-Free Galerkin Method. *International Journal of Computational Methods*, **5**(1): 91–117.

Shahid, I. and Chang, F.-K. (1995). An accumulative damage model for tensile and shear failures of laminated composite plates. *Journal of Composite Materials*, **29**: 926–956.

Shao, J. F., Chau, K. T., and Feng, X. T. (2006). Modeling of anisotropic damage and creep deformation in brittle rocks. *International Journal of Rock Mechanics & Mining Sciences*, **43**: 582–592.

Shao, J. F., Zhou, H., and Chau, K. T. (2005). Coupling between anisotropic damage and permeability variation in brittle rocks. *Int. J. Numer. Anal. Meth. Geomech.*, **29**: 1231–1247.

Suzuki T. (2012). Understanding of dynamic earthquake slip behavior using damage as a tensor variable: Microcrack distribution, orientation, and mode and secondary faulting. *Journal of Geophysical Research*, **B5**: 1–20.

Swoboda, G. and Yang, Q. (1999). An energy-based damage model of geomaterials. I. Formulation and numerical results. *International Journal of Solids and Structures*, **36**: 1719–1734.

Tvergaard, V. and Nielsen, K. L. (2010). Relations between a micro-mechanical model and a damage model for ductile failure in shear. *Journal of the Mechanics and Physics of Solids*, **58**: 1243–1252.

Valko, P. and Economides, M.J. (1994). Propagation of Hydraulically Induced Fractures a Continuum Damage Mechanics Approach. *International Journal of Rock Mechanics and Mining Sciences & Geomechanics Abstracts*, **31**(3): 221–229.

Vardoulakis, I. and Sulem, J. Second-grade plasticity theory for geomaterials. in: *Bifurcation Analysis in Geomechanics*, Blackie Academic and Professional, 2005, Chap.10, pp. 282–425.

Yu, H.S. (2006). Plasticity and Geotechnics. *Springer*.

Zhou, J. J., Shao, J. F., and Xu, W. Y. (2006). Coupled modeling of damage growth and permeability variation in brittle rocks. *Mechanics Research Communications*, **33**: 450–459.

Zhu Q., Kondo, D., Shao, J.-F. (2007) An Homogenization-Based Nonlocal Damage Model for Brittle Materials and Applications. *ICCS 2007, Part III, LNCS 4489, Springer-Verlag, Shi et al. (eds)*, 1130–1137.